

# Thermo-mechanical vibration analysis of a single-walled carbon nanotube embedded in an elastic medium based on higher-order shear deformation beam theory<sup>†</sup>

Farzad Ebrahimi\* and Erfan Salari

*Department of Mechanical Engineering, Faculty of Engineering, Imam Khomeini International University, Qazvin, Iran*

(Manuscript Received January 7, 2015; Revised March 16, 2015; Accepted March 30, 2015)

## Abstract

In this study, the thermal effect on the free vibration characteristics of embedded Single-walled carbon nanotubes (SWCNTs) based on the size-dependent Reddy higher order shear deformation beam theory subjected to in-plane thermal loading is investigated by presenting a Navier-type solution and employing a semi-analytical Differential transform method (DTM) for the first time. In addition, the exact nonlocal Reddy beam theory solution presented here should be useful to engineers designing nanoelectromechanical devices. The small-scale effect is considered based on nonlocal elasticity theory of Eringen. The nonlocal equations of motion are derived through Hamilton's principle, and they are solved by applying DTM. Numerical results reveal that the proposed modeling and semi-analytical approach can provide more accurate frequency results of the SWCNTs compared to analytical results and some cases in the literature. The detailed mathematical derivations are presented, and numerical investigations are performed, whereas emphasis is placed on investigating the effect of several parameters such as small-scale effects, boundary conditions, mode number, thickness ratio, temperature change, and Winkler spring modulus on the natural frequencies of the SWCNTs in detail. The vibration behavior of SWCNTs is significantly influenced by these effects. Results indicate that the inclusion of size effect results in a decrease in nanobeam stiffness and leads to a decrease in natural frequency. Numerical results are presented to serve as benchmarks for future analyses of SWCNTs.

*Keywords:* Differential transformation method; Nonlocal elasticity; Reddy beam theory; SWCNT; Thermo-mechanical vibration

## 1. Introduction

Nanoscale engineering materials have attracted great interest in modern science and technology after the invention of Carbon nanotubes (CNTs) by Iijima [1]. They are characterized by significant mechanical, thermal, and electrical performances that are superior to conventional structural materials. In recent years, nanobeams and CNTs hold a wide variety of potential applications [2, 3] such as sensors, actuators, transistors, probes, and resonators in Nano-electro-mechanical system (NEMS). Continuum mechanics offers an easy and useful tool for the analysis of CNTs because conducting experiments at the nanoscale is a daunting task and atomistic modeling is restricted to small-scale systems owing to computer resource limitations. However, classical continuum models need to be extended to consider the nanoscale effects, and this extension can be achieved by nonlocal elasticity theory proposed by Eringen [4], which considers the size-dependent effect.

Furthermore, with the development of material technology,

Single-walled carbon nanotubes (SWCNTs) have been employed in Micro/Nano-electro-mechanical systems (MEMS/NEMS) [5]. Understanding their mechanical properties and vibration behavior is significant in their design and manufacture because of the high sensitivity of these systems to external stimulations. Thus, establishing an accurate model of nanobeams is a key issue for successful NEMS design. Peddieson et al. [6] proposed a version of nonlocal elasticity theory employed to develop a nonlocal Euler beam model. The thermo-mechanical vibration of short CNTs embedded in Pasternak foundation was presented by Amirian et al. [7] based on nonlocal elasticity theory. They also concluded that the high temperature change and nonlocal parameter play important roles in the vibrational response of the CNTs. Murmu and Pradhan [8] used Euler-Bernoulli beam theory (EBT) to investigate thermo-mechanical vibration analysis of SWCNTs embedded in an elastic medium. They noticed that small-scale effects are significant in the vibration response of a SWCNT. Zhang et al. [9] studied the thermal effect on the vibration of double-walled CNTs based on thermal elasticity mechanics and nonlocal elasticity theory. Wang et al. [10] exploited the thermal effect on the vibration and instability of conveying fluid SWCNTs based on the Euler beam. Through

\*Corresponding author. Tel.: +98 28 33780021, Fax.: +98 28 33780084  
E-mail address: febrahimi@eng.ikiu.ac.ir

<sup>†</sup>Recommended by Associate Editor Heung Soo Kim

© KSME & Springer 2015

the Galerkin method, the transverse vibration of embedded SWCNTs with light waviness based on nonlocal Euler-Bernoulli and Timoshenko beam models is studied by Soltani et al. [11]. Most of the recent studies on SWCNTs have been conducted based on EBT and Timoshenko beam theory (TBT). However, the effects of rotary inertia and shear deformation are neglected in EBT, so EBT always overestimates buckling load and natural frequency of free vibration and underestimates deflection. Moreover, in TBT, a shear correction factor is required to compensate for the difference between the actual stress state and the constant stress state. In avoiding the use of shear correction factor and obtaining a better prediction of the response of a deep beam, many higher-order shear deformation theories have been developed, such as the third-order shear deformation theory proposed by Reddy [12], which presents a more realistic model of the beam in the determination of higher modes of vibration. To the author's best knowledge, no work has reported on the application of the Differential transform method (DTM) on the thermo-mechanical vibration analysis of embedded SWCNTs within the framework of Reddy higher order beam theory (RHOB). In this study, the non-classical third-order shear deformation beam model is developed, and governing equations and boundary conditions for the free vibration of a nonlocal embedded SWCNT have been derived through Hamilton's principle. A new semi-analytical method called DTM is employed for the vibration analysis of size-dependent SWCNTs with four combinations of boundary conditions for the first time. The superiority of the DTM is found in its simplicity and good precision and depends on the Taylor series expansion, and it takes less time to solve polynomial series. With this method, obtaining highly accurate results or exact solutions for differential equations is possible. The detailed mathematical derivations are presented, and numerical investigations are performed, whereas emphasis is placed on investigating the effects of several parameters such temperature change, mode number, thickness ratios, boundary conditions, Winkler spring modulus, and small-scale parameter on the vibration characteristics of SWCNTs. Comparisons of the results with those from the existing literature are provided, and the good agreement between the two sets of results validated the presented approach.

**2. Theory and formulation**

**2.1. Nonlocal elasticity model for SWCNT**

In the classic elastic continuum theory, the stress field at a point  $x$  only depends on the strain field at the same point. However, according to Eringen's nonlocal elasticity theory [13], the stress field at a point is dependent on the strains at all other points in the body. Therefore, the nonlocal stress tensor  $\sigma_{ij}$  at point  $x$  is defined by the following:

$$\sigma_{ij}(x) = \int_{\Omega} \alpha(|x' - x|, \tau) t_{ij}(x') d\Omega(x') \tag{1}$$

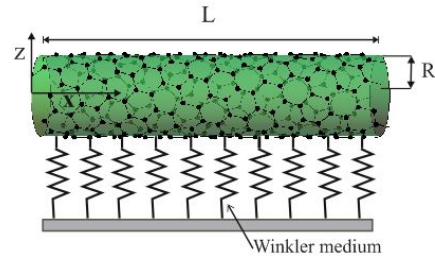


Fig. 1. Schematic of embedded SWCNT.

$$t_{ij} = C_{ijkl} \epsilon_{kl} \tag{2}$$

where  $t_{ij}(x')$  is the classical macroscopic stress tensor at point  $x$ , the kernel function  $\alpha(|x' - x|, \tau)$  is the nonlocal modulus,  $|x' - x|$  is the distance, and  $\tau$  is a material constant that depends on type of material.  $t_{ij}$  is the macroscopic stress tensor at a point  $x$  in a Hookean solid, which is dependent on the strain  $\epsilon$  at the same point according to generalized Hooke's law.  $C$  is the fourth-order elasticity tensor. A simplified equation of differential form is used as a basis of nonlocal constitutive formulation because solving the integral constitutive Eqs. (1) and (2) are complicated:

$$(1 - (e_0 a)^2 \nabla^2) \sigma_{kl} = t_{kl} \tag{3}$$

where  $\nabla^2$  is the Laplacian operator. The scale length  $e_0 a$  considers the size effect on the response of nanostructures. The nonlocal parameter  $e_0 a$  is experimentally obtained for various materials. Thus, in the present study, a conservative estimate of the nonlocal parameter  $(e_0 a)^2$  for SWCNT is considered in the range of 0-4 (nm)<sup>2</sup> [8]. For an elastic material, the nonlocal constitutive relations may be simplified as the following:

$$\sigma_{xx} - \mu \frac{\partial^2 \sigma_{xx}}{\partial x^2} = E(\epsilon_{xx} - \alpha_x T) \tag{4}$$

$$\sigma_{xz} - \mu \frac{\partial^2 \sigma_{xz}}{\partial x^2} = G \gamma_{xz} \tag{5}$$

where  $\sigma$  and  $\epsilon$  are the nonlocal stress and strain, respectively,  $\mu = (e_0 a)^2$  is the nonlocal parameter,  $E$  is the elasticity modulus,  $G = E / 2(1 + \nu)$  is the shear modulus, and  $\nu$  is Poisson's ratio.  $\alpha_x$  and  $T$  are the thermal expansion and temperature change, respectively.

**2.2 Kinematic relations**

As shown in Fig. 1, a SWCNT is modeled as a higher order beam with length  $L$  and circular cross-section of radius  $R$ , where the  $x$  axis is taken along the central axis, and the  $z$ -axis is considered in the width direction. The SWCNT vibrates only in the  $x$ - $z$  plane. Based on RHOB, the displace-

ment of an arbitrary point in the beam along the  $x$ - and  $z$ -axes, denoted by  $\tilde{U}(x, z, t)$  and  $\tilde{W}(x, z, t)$ , respectively, is the following [14]:

$$\tilde{U}(x, z, t) = z\varphi(x, t) - \frac{4z^3}{3h^2} \left( \varphi(x, t) + \frac{\partial w(x, t)}{\partial x} \right) \quad (6)$$

$$\tilde{W}(x, z, t) = w(x, t) \quad (7)$$

where  $t$  is time,  $w$  and  $\varphi$  are the transverse displacement and angular displacement of the cross-sections at any point on the neutral axis of the beam, respectively. Based on Eqs. (6) and (7), the nonzero strains of the Reddy beam theory can be obtained as the following:

$$\varepsilon_{xx} = z \frac{\partial \varphi}{\partial x} - \frac{4z^3}{3h^2} \left( \frac{\partial \varphi}{\partial x} + \frac{\partial^2 w}{\partial x^2} \right) \quad (8)$$

$$\gamma_{xz} = \left( \varphi + \frac{\partial w}{\partial x} \right) \left( 1 - \frac{4z^2}{h^2} \right). \quad (9)$$

In defining the nonlocal stress resultants,  $M, P, Q$ , and  $R$  are defined as the following:

$$\begin{aligned} M &= \int_A z \sigma_{xx} dA, & P &= \int_A z^3 \sigma_{xx} dA \\ Q &= \int_A \sigma_{xz} dA, & R &= \int_A z^2 \sigma_{xz} dA \end{aligned} \quad (10)$$

where  $\sigma_{xx}$  and  $\sigma_{xz}$  are the normal and shear stresses, respectively. Through Eqs. (8)-(10), based on Hamilton's principle [15] and nonlocal elasticity theory, the governing equations are obtained as the following:

$$\frac{\partial M}{\partial x} - \frac{4}{3h^2} \frac{\partial P}{\partial x} - Q + \frac{4}{h^2} R = \frac{68\rho I}{105} \frac{\partial^2 \varphi}{\partial t^2} - \frac{16\rho I}{105} \frac{\partial^3 w}{\partial t^2 \partial x} \quad (11)$$

$$\begin{aligned} \frac{4}{3h^2} \frac{\partial^2 P}{\partial x^2} + \frac{\partial Q}{\partial x} - \frac{4}{h^2} \frac{\partial R}{\partial x} + N_{Temp} \frac{\partial^2 w}{\partial x^2} \\ - K_w w = \rho A \frac{\partial^2 w}{\partial t^2} - \frac{\rho I}{21} \frac{\partial^4 w}{\partial t^2 \partial x^2} + \frac{16\rho I}{105} \frac{\partial^3 \varphi}{\partial t^2 \partial x} \end{aligned} \quad (12)$$

where  $K_w$  is the Winkler modulus and  $N_{Temp}$  is the thermally induced axial force derived from the constitutive relationship between the thermal strain and thermal stress as follows [15]:

$$N_{Temp} = -EA\alpha_x T. \quad (13)$$

Furthermore, the following boundary conditions at the edges of the nanobeam ( $x = 0, L$ ) are obtained as follows:

$$\frac{4}{3h^2} P - M = 0 \quad \text{or} \quad \varphi = 0 \quad (14)$$

$$\frac{-4}{3h^2} \frac{\partial P}{\partial x} + \frac{4}{h^2} R - Q - \frac{\rho I}{21} \frac{\partial^3 w}{\partial t^2 \partial x} + \frac{16\rho I}{105} \frac{\partial^2 \varphi}{\partial t^2} = 0 \quad \text{or}$$

$$w = 0 \quad (15)$$

$$\frac{4}{3h^2} P = 0 \quad \text{or} \quad \frac{\partial w}{\partial x} = 0. \quad (16)$$

The integration of Eqs. (4) and (5) constitutive equations of nonlocal elasticity for a nanobeam may be written as the following:

$$M - \mu \frac{\partial^2 M}{\partial x^2} = \frac{EI}{5} \left( 4 \frac{\partial \varphi}{\partial x} - \frac{\partial^2 w}{\partial x^2} \right) \quad (17a)$$

$$P - \mu \frac{\partial^2 P}{\partial x^2} = \frac{EAh^4}{1680} \left( 16 \frac{\partial \varphi}{\partial x} - 5 \frac{\partial^2 w}{\partial x^2} \right) \quad (17b)$$

$$Q - \mu \frac{\partial^2 Q}{\partial x^2} = \frac{2GA}{3} \left( \varphi + \frac{\partial w}{\partial x} \right) \quad (17c)$$

$$R - \mu \frac{\partial^2 R}{\partial x^2} = \frac{2GI}{5} \left( \varphi + \frac{\partial w}{\partial x} \right). \quad (17d)$$

As a final point, the nonlocal governing equations in terms of the displacement can be written by substituting  $M, P, Q$ , and  $R$  from Eq. (17) into Eqs. (11) and (12) as follows:

$$\begin{aligned} \frac{16EI}{105} \frac{\partial^3 w}{\partial x^3} + \frac{8GA}{15} \frac{\partial w}{\partial x} - \frac{68EI}{105} \frac{\partial^2 \varphi}{\partial x^2} \\ + \frac{8GA}{15} \varphi = \mu \left( \frac{68\rho I}{105} \frac{\partial^4 \varphi}{\partial t^2 \partial x^2} - \frac{16\rho I}{105} \frac{\partial^5 w}{\partial t^2 \partial x^3} \right) \\ + \frac{16\rho I}{105} \frac{\partial^3 w}{\partial t^2 \partial x} - \frac{68\rho I}{105} \frac{\partial^2 \varphi}{\partial t^2} \\ - \frac{EI}{21} \frac{\partial^4 w}{\partial x^4} + \frac{8GA}{15} \frac{\partial^2 w}{\partial x^2} + \frac{16EI}{105} \frac{\partial^3 \varphi}{\partial x^3} + \frac{8GA}{15} \frac{\partial \varphi}{\partial x} \\ - EA\alpha_x T \left( \frac{\partial^2 w}{\partial x^2} - \mu \frac{\partial^4 w}{\partial x^4} \right) - K_w \left( w - \mu \frac{\partial^2 w}{\partial x^2} \right) \\ = \mu \left( \frac{\rho I}{21} \frac{\partial^6 w}{\partial t^2 \partial x^4} - \rho A \frac{\partial^4 w}{\partial t^2 \partial x^2} - \frac{16\rho I}{105} \frac{\partial^5 \varphi}{\partial t^2 \partial x^3} \right) \\ + \rho A \frac{\partial^2 w}{\partial t^2} - \frac{\rho I}{21} \frac{\partial^4 w}{\partial t^2 \partial x^2} + \frac{16\rho I}{105} \frac{\partial^3 \varphi}{\partial t^2 \partial x} \end{aligned} \quad (18)$$

### 3. Solution method

#### 3.1 Analytical solution

Here, based on the Navier-type solution method for the free vibration of a simply supported SWCNT, the displacement functions are expressed as the product of undetermined coefficients and known trigonometric functions to satisfy the governing equations and the conditions at  $x = 0, L$ . The following displacement fields are assumed to be of the form:

$$w(x, t) = \sum_{n=1}^{\infty} W_n \sin\left(\frac{n\pi}{L}x\right) e^{i\omega_n t} \quad (20a)$$

$$\varphi(x, t) = \sum_{n=1}^{\infty} \phi_n \cos\left(\frac{n\pi}{L}x\right) e^{i\omega_n t}. \quad (20b)$$

where  $(W_n, \phi_n)$  are the unknown Fourier coefficients to be determined for each  $n$  value. By substituting Eq. (20) into Eqs. (18) and (19) and setting the determinant of the coefficient matrix, the analytical solutions can be obtained from the following equation:

$$\{[K] - \omega^2[M]\} \begin{Bmatrix} W_n \\ \phi_n \end{Bmatrix} = 0 \tag{21}$$

where  $[K]$  and  $[M]$  are the stiffness matrix and mass matrix, respectively. By setting the determinant of the coefficient matrix, one obtains a quadratic polynomial for  $\omega_n^2$ , and then by setting this polynomial to zero, one can find  $\omega_n$ .

### 3.2 Implementation of DTM

Some of the common numerical methods used to solve the initial- and boundary-value problems occurring in engineering are homotopy perturbation method, variational iteration method, parameter-expanding methods, and others [16]. Moreover, the principle of DTM is to transform the differential equations of governing and boundary equations into a set of algebraic equations using Taylor series expansion with transformation rules. The details of DTM have been described elsewhere [17]. Therefore, the elaborate information on this aspect is not attempted here. Based on the basic transformation operations introduced in Table 1, the transformed form of the governing Eqs. (18) and (19) may be obtained as the following:

$$\begin{aligned} & \left( \frac{16EI}{105} - \mu \frac{16\rho I \omega^2}{105} \right) \frac{(k+3)!}{k!} W[k+3] \\ & + \left( \frac{8GA}{15} + \frac{16\rho I \omega^2}{105} \right) \frac{(k+1)!}{k!} W[k+1] \\ & + \left( \mu \frac{68\rho I \omega^2}{105} - \frac{68EI}{105} \right) \frac{(k+2)!}{k!} \phi[k+2] \\ & + \left( \frac{8GA}{15} - \frac{68\rho I \omega^2}{105} \right) \phi[k] = 0 \end{aligned} \tag{22}$$

$$\begin{aligned} & \left( \frac{-EI}{21} + \mu(EA\alpha_x T) + \mu \frac{\rho I \omega^2}{21} \right) \frac{(k+4)!}{k!} W[k+4] \\ & + \left( \frac{8GA}{15} - EA\alpha_x T + \mu K_w - \mu \rho A \omega^2 - \frac{\rho I \omega^2}{21} \right) \frac{(k+2)!}{k!} W[k+2] \\ & + (\rho A \omega^2 - K_w) W[k] + \left( \frac{16EI}{105} - \mu \frac{16\rho I \omega^2}{105} \right) \frac{(k+3)!}{k!} \phi[k+3] \\ & + \left( \frac{16\rho I \omega^2}{105} + \frac{8GA}{15} \right) \frac{(k+1)!}{k!} \phi[k+1] = 0 \end{aligned} \tag{23}$$

where  $\phi[k]$  and  $W[k]$  are the transformed functions of  $\phi$  and  $w$ , respectively. By employing DTM theorems into Eqs.

Table 1. Some of the transformation rules of DTM.

| Original function              | Transformed function              |
|--------------------------------|-----------------------------------|
| $f(x) = g(x) \pm h(x)$         | $F(K) = G(K) \pm H(K)$            |
| $f(x) = \lambda g(x)$          | $F(K) = \lambda G(K)$             |
| $f(x) = \frac{d^n g(x)}{dx^n}$ | $F(K) = \frac{(k+n)!}{k!} G(K+n)$ |

(14)-(16), the transformed boundary conditions are obtained. For instance, the transformed simply supported edge condition can be given as the following:

$$W[0] = 0, \frac{68}{105} \phi[1] - \frac{16}{105} W[2] = 0 \tag{24}$$

$$\sum_{k=0}^{\infty} W[k] = 0, \frac{68}{105} \sum_{k=0}^{\infty} k \phi[k] - \frac{16}{105} \sum_{k=0}^{\infty} k(k-1) W[k] = 0.$$

By using Eqs. (22) and (23) together with the transformed boundary conditions, one arrives at the following eigenvalue problem:

$$\begin{bmatrix} M_{11}(\omega) & M_{12}(\omega) & M_{13}(\omega) \\ M_{21}(\omega) & M_{22}(\omega) & M_{23}(\omega) \\ M_{31}(\omega) & M_{32}(\omega) & M_{33}(\omega) \end{bmatrix} [C] = 0 \tag{25}$$

where  $[c]$  corresponds to the missing boundary conditions at  $x = 0$ . For the non-trivial solutions of Eq. (25), the determinant of the coefficient matrix should be equal to zero. In solving Eq. (25), the  $i$ th estimated eigenvalue for  $n$ th iteration ( $\omega = \omega_i^{(n)}$ ) may be obtained, and the total number of iterations is related to the accuracy of the calculations, which can be determined by the following equation:

$$|\omega_i^{(n)} - \omega_i^{(n-1)}| < \varepsilon. \tag{26}$$

In this study,  $\varepsilon = 0.0001$  is considered in the process of determining eigenvalues, resulting in a four-digit precision in the estimated eigenvalues.

### 4. Convergence and correctness of the method

Through this section, a numerical testing of the procedure will be performed, and the effects of several parameters on the natural frequencies of the SWCNT will be identified. The effective properties of SWCNT are taken as that of Reddy and Pang [18]. The Young's modulus  $E = 1000$  GPa, mass density  $\rho = 2300$  Kg/m<sup>3</sup>, Poisson's ratio  $\nu = 0.19$ , and diameter  $d = 1$  nm are considered in the analysis. As indicated by Jiang et al. [19], the coefficients of thermal expansion for CNTs are negative at a lower temperature and become positive at a higher temperature; for the case of room or low temperature, we suppose a  $\alpha_x = -1.6 \cdot 10^{-6}$  1/K [20]. The following relation is

Table 2. Convergence study for the first three natural frequencies of S-S SWCNT ( $L/d = 50, \mu = 3 \text{ nm}^2, T = 30 \text{ K}$ ).

| Method     | $k$     | $\hat{\omega}_1$ | $\hat{\omega}_2$ | $\hat{\omega}_3$ |
|------------|---------|------------------|------------------|------------------|
| DTM        | 10      | 10.5517          | -                | -                |
|            | 12      | 10.7477          | -                | -                |
|            | 14      | 10.7280          | -                | -                |
|            | 16      | 10.7293          | 37.3927          | -                |
|            | 18      | 10.7292          | 40.0444          | -                |
|            | 20      | 10.7292          | 39.4259          | -                |
|            | 22      | 10.7292          | 39.4904          | -                |
|            | 24      | 10.7292          | 39.4841          | -                |
|            | 26      | 10.7292          | 39.4846          | 84.2696          |
|            | 28      | 10.7292          | 39.4846          | 85.2870          |
|            | 30      | 10.7292          | 39.4846          | 85.1365          |
|            | 32      | 10.7292          | 39.4846          | 85.1528          |
|            | 34      | 10.7292          | 39.4846          | 85.1512          |
|            | 36      | 10.7292          | 39.4846          | 85.1513          |
|            | 38      | 10.7292          | 39.4846          | 85.1513          |
|            | 40      | 10.7292          | 39.4846          | 85.1513          |
| 42         | 10.7292 | 39.4846          | 85.1513          |                  |
| 44         | 10.7292 | 39.4846          | 85.1513          |                  |
| Analytical |         | 10.7288          | 39.4725          | 85.0864          |

Table 3. Comparison of non-dimensional fundamental frequencies of S-S SWCNT ( $L/d = 10$ ).

| $\mu = (e_0 a)^2$ | Analytical [12] | Present DTM |
|-------------------|-----------------|-------------|
| 0                 | 9.7454          | 9.7360      |
| 1                 | 9.2974          | 9.2885      |
| 2                 | 8.9060          | 8.8974      |
| 3                 | 8.5602          | 8.5520      |
| 4                 | 8.2517          | 8.2438      |

performed to calculate the non-dimensional natural frequencies:

$$\hat{\omega} = \omega L^2 \sqrt{\rho A / EI} \tag{27}$$

where  $I$  is the moment of inertia of the cross section of the nanotube. It is found that in DTM after a certain number of iterations eigenvalues converged to a value with good precision, so the number of iterations is important in DTM convergence. Table 2 tabulates the convergence study for the first three natural frequencies of the simply supported SWCNT. As seen in Table 2, the third natural frequency converged after 38 iterations with 4-digit precision, whereas the first and second ones converged after 20 and 28 iterations, respectively. To evaluate the accuracy of the natural frequencies predicted by the present method, Table 3 compares the semi-analytical results of the present study and the results obtained for the simply supported SWCNT with different nonlocal parameters

(varying from 0 to 4) and length-to-thickness ratios ( $L/d = 10$ ) presented by Reddy [12], which has been obtained by the analytical method. The parameters used in this table are the following [12]:  $L = 10, E = 30 * 10^6, \rho = 1, \nu = 0.3$ . One may clearly notice that the non-dimensional fundamental frequency parameters obtained in the present investigation are in excellent agreement to the results presented by Reddy [12] for all compared cases and validate the proposed method of solution.

### 5. Numerical results and discussions

After the approaches are validated, some parametric studies are conducted in this section to examine the influences of various parameters such as nonlocal parameters, length-to-thickness ratios, temperature changes, and boundary conditions on the natural frequencies of the SWCNT. Four different combinations of edge conditions at  $x=0, L$  are considered as: simply-supported/simply-supported (S-S), clamped/simply-supported (C-S), clamped/clamped (C-C), and clamped/free (C-F). In Table 4, the first three dimensionless frequencies of the S-S SWCNT are presented for the various values of the aspect ratios ( $L/d = 10, 50$ ) and nonlocal parameters ( $\mu = 0, 1, 2, 3, 4$ ) for low temperature change ( $T = 30 \text{ K}$ ) based on both DTM and analytical Navier solution method. First, when the nonlocal parameter vanishes, Reddy's classical isotropic beam theory is rendered. An increase in nonlocal scale parameter gives rise to a decrement in the first three dimensionless frequencies because the presence of the nonlocal effect tends to decrease the stiffness of the nanostructures and hence decreases the values of natural frequencies. The dimensionless natural frequencies predicted by DTM are in close agreement with those evaluated through analytical solution. Moreover, the first three dimensionless natural frequencies increase by increasing aspect ratio ( $L/d$ ). In investigating the effects of different boundary conditions and nonlocal parameters on the vibration characteristics of SWCNT, the non-dimensional frequencies of SWCNT under low temperature change ( $T = 50 \text{ K}$ ) with different edge conditions (i.e., C-C, C-S, and C-F) are tabulated in Table 5. This table shows that frequencies predicted by the nonlocal solution are smaller than those of the local frequency because of the small-scale effects. For this reason, the size effect plays a major role in the vibration behavior of CNTs. Moreover, for a C-F SWCNT, increasing the nonlocal parameter leads to an increase in fundamental frequency. Furthermore, a beam with stiffer edges, such as C-C and C-S, shows higher natural frequencies than those of other boundary conditions, as expected. The fundamental frequency parameter as a function of aspect ratio and temperature increase is presented in Fig. 2 for the S-S SWCNT with different nonlocal parameters. Similarly, the variation of the first dimensionless frequency with temperature change for different nonlocality is depicted in Fig. 3. Observing these two figures shows that increasing the nonlocality parameter yields the reduction in dimensionless frequencies for all temperature changes and aspect ratios, which highlights the significance of

Table 4. Effects of nonlocality parameters and aspect ratios on the first three dimensionless frequencies of S-S SWCNT ( $T = 30\text{K}$ ).

| L/d | $\mu = (e_0 a)^2$ | Present          | Present    | Present          | Present    | Present          | Present    |
|-----|-------------------|------------------|------------|------------------|------------|------------------|------------|
|     |                   | DTM              | Analytical | DTM              | Analytical | DTM              | Analytical |
|     |                   | $\hat{\omega}_1$ |            | $\hat{\omega}_2$ |            | $\hat{\omega}_3$ |            |
| 10  | 0                 | 9.8147           | 9.7932     | 38.0899          | 37.7910    | 82.0930          | 80.9035    |
|     | 1                 | 9.3670           | 9.3466     | 32.2645          | 32.0120    | 59.7655          | 58.9018    |
|     | 2                 | 8.9761           | 8.9566     | 28.4951          | 28.2729    | 49.3061          | 48.5961    |
|     | 3                 | 8.6309           | 8.6121     | 25.8018          | 25.6012    | 42.9333          | 42.3175    |
|     | 4                 | 8.3231           | 8.3050     | 23.7542          | 23.5701    | 38.5332          | 37.9827    |
| 50  | 0                 | 10.7822          | 10.7818    | 40.3648          | 40.3522    | 89.4739          | 89.4050    |
|     | 1                 | 10.7644          | 10.7640    | 40.0644          | 40.0520    | 87.9585          | 87.8910    |
|     | 2                 | 10.7468          | 10.7464    | 39.7711          | 39.7589    | 86.5197          | 86.4535    |
|     | 3                 | 10.7292          | 10.7288    | 39.4846          | 39.4725    | 85.1513          | 85.0864    |
|     | 4                 | 10.7118          | 10.7114    | 39.2046          | 39.1926    | 83.8478          | 83.7840    |

Table 5. Effect of different boundary conditions on the first three dimensionless frequencies of SWCNT ( $T = 50\text{K}$ ).

| L/d | $\mu = (e_0 a)^2$ | Boundary conditions |                  |                  |                  |                  |                  |                  |                  |                  |
|-----|-------------------|---------------------|------------------|------------------|------------------|------------------|------------------|------------------|------------------|------------------|
|     |                   | C-C                 |                  |                  | C-S              |                  |                  | C-F              |                  |                  |
|     |                   | $\hat{\omega}_1$    | $\hat{\omega}_2$ | $\hat{\omega}_3$ | $\hat{\omega}_1$ | $\hat{\omega}_2$ | $\hat{\omega}_3$ | $\hat{\omega}_1$ | $\hat{\omega}_2$ | $\hat{\omega}_3$ |
| 10  | 0                 | 22.1465             | 59.1398          | 110.8100         | 15.2966          | 48.0657          | 95.9430          | 3.5033           | 21.7941          | 59.1722          |
|     | 1                 | 20.8464             | 48.4212          | 77.1223          | 14.4800          | 40.0684          | 68.3604          | 3.5202           | 20.4085          | 48.5095          |
|     | 2                 | 19.7498             | 41.9787          | 62.7322          | 13.7814          | 35.0894          | 56.0132          | 3.5376           | 19.2244          | 42.1439          |
|     | 3                 | 18.8092             | 37.5709          | 54.2844          | 13.1751          | 31.6129          | 48.6279          | 3.5553           | 18.1958          | 37.8274          |
|     | 4                 | 17.9913             | 34.3152          | 48.5681          | 12.6428          | 29.0103          | 43.5794          | 3.5734           | 17.2902          | 34.6722          |
| 50  | 0                 | 23.2232             | 62.7430          | 121.7400         | 16.5587          | 51.2340          | 105.2980         | 3.1556           | 22.9575          | 62.7638          |
|     | 1                 | 23.1801             | 62.2102          | 119.4670         | 16.5300          | 50.8304          | 103.4330         | 3.1584           | 22.9112          | 62.2324          |
|     | 2                 | 23.1373             | 61.6917          | 117.3210         | 16.5016          | 50.4371          | 101.6680         | 3.1613           | 22.8653          | 61.7153          |
|     | 3                 | 23.0948             | 61.1868          | 115.2910         | 16.4733          | 50.0537          | 99.9940          | 3.1642           | 22.8197          | 61.2119          |
|     | 4                 | 23.0527             | 60.6950          | 113.3670         | 16.4452          | 49.6798          | 98.4040          | 3.1670           | 22.7744          | 60.7217          |

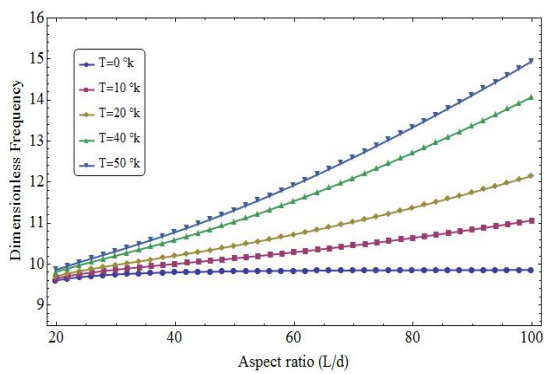


Fig. 2. Variation of the first dimensionless frequency of S-S SWCNT versus aspect ratio ( $L/d$ ) for different low temperatures ( $\mu = 2$ ).

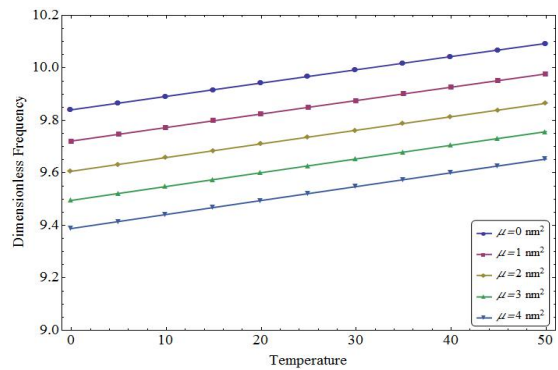


Fig. 3. Variation of first dimensionless frequency of S-S SWCNT versus temperature change for different nonlocal parameters ( $L/d = 20$ ).

the nonlocal effect. In addition, the fundamental frequency increases by increasing temperature changes, and temperature change has a significant effect on the fundamental frequency of the S-S SWCNT.

Finally, Fig. 4 displays the variations of the first dimensionless natural frequency of the S-S SWCNT with respect to

Winkler spring modulus for different values of nonlocal parameters at a constantly low temperature ( $T = 40\text{K}$ ) and aspect ratio ( $L/d = 10$ ). The figure shows that the fundamental frequency of SWCNT increases with the increase of Winkler spring modulus. In addition, the small-scale parameter has a softening effect on SWCNT.

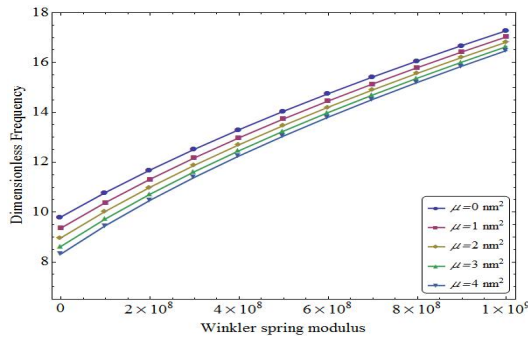


Fig. 4. Variation of the first dimensionless frequency of S-S SWCNT versus Winkler spring modulus for different nonlocal parameters ( $L/d = 10$ ,  $T = 40$  K).

## 6. Conclusions

The vibrational behavior of embedded SWCNTs subjected to thermal loading with various boundary conditions is investigated based on the Reddy beam theory in conjunction with DTM. Eringen's theory of nonlocal elasticity together with higher order beam theory is used to model the CNT by the implementation of Hamilton's principle. The accuracy of the results is examined using available data in the literature. Finally, through some parametric studies and numerical examples, various factors such as nonlocal parameter, temperature change, boundary conditions, and Winkler spring modulus are found to play important roles in the dynamic behavior of SWCNTs. The nanobeam model produces a smaller natural frequency than the classical (local) beam model. Therefore, the small-scale effects should be considered in the analysis of the mechanical behavior of nanostructures. The dimensionless frequency decreases with the increase in temperature. Moreover, under an increase in temperature, an increase in the Winkler spring modulus results in an increase in frequency.

## References

- [1] S. Iijima, Helical microtubules of graphitic carbon, *Nature*, 354 (6348) (1991) 56-58.
- [2] Y. Q. Zhang, G. R. Liu and J. S. Wang, Small-scale effects on buckling of multiwalled carbon nanotubes under axial compression, *Physical review B*, 70 (20) (2004) 205430.
- [3] Q. Wang and V. K. Varadan, Vibration of carbon nanotubes studied using nonlocal continuum mechanics, *Smart Materials and Structures*, 15 (2) (2006) 659.
- [4] A. C. Eringen, Nonlocal polar elastic continua, *International Journal of Engineering Science*, 10 (1) (1972) 1-16.
- [5] Z. Lee, C. Ophus, L. M. Fischer, N. Nelson-Fitzpatrick, K. L. Westra, S. Evoy, V. Radmilovic, U. Dahmen and D. Mitlin, Metallic NEMS components fabricated from nanocomposite Al-Mo films, *Nanotechnology*, 17 (12) (2006) 3063.
- [6] J. Peddieson, G. R. Buchanan and R. P. McNitt, Application of nonlocal continuum models to nanotechnology, *International Journal of Engineering Science*, 41 (3) (2003) 305-312.
- [7] B. Amirian, R. Hosseini-Ara and H. Moosavi, Thermo-mechanical vibration of short carbon nanotubes embedded in pasternak foundation based on nonlocal elasticity theory, *Shock and Vibration*, 20 (4) (2013) 821-832.
- [8] T. Murmu and S. C. Pradhan, Thermo-mechanical vibration of a single-walled carbon nanotube embedded in an elastic medium based on nonlocal elasticity theory, *Computational Materials Science*, 46 (4) (2009) 854-859.
- [9] Y. Q. Zhang, X. Liu and G. R. Liu, Thermal effect on transverse vibrations of double-walled carbon nanotubes, *Nanotechnology*, 18 (44) (2007) 445701.
- [10] L. Wang, Q. Ni, M. Li and Q. Qian, The thermal effect on vibration and instability of carbon nanotubes conveying fluid, *Physica E: Low-dimensional Systems and Nanostructures*, 40 (10) (2008) 3179-3182.
- [11] P. Soltani, A. Kassaei, M. M. Taherian and A. Farshidianfar, Vibration of wavy single-walled carbon nanotubes based on nonlocal Euler Bernoulli and Timoshenko models, *International Journal of Advanced Structural Engineering (IJASE)*, 4 (1) (2012) 1-10.
- [12] J. N. Reddy, Nonlocal theories for bending, buckling and vibration of beams, *International Journal of Engineering Science*, 45 (2) (2007) 288-307.
- [13] A. C. Eringen and D. G. B. Edelen, On nonlocal elasticity, *International Journal of Engineering Science*, 10 (3) (1972) 233-248.
- [14] P. R. Heyliger and J. N. Reddy, A higher order beam finite element for bending and vibration problems, *Journal of Sound and Vibration*, 126 (2) (1998) 309-326.
- [15] J. X. Huang, M. F. Song, H. Y. Kong, P. Wang and J. H. He, Effect of temperature on non-linear dynamical property of stuffer box crimping and bubble electrospinning, *Thermal Science*, 18 (3) (2014) 1049-1053.
- [16] J. H. He, Some asymptotic methods for strongly nonlinear equations, *International Journal of Modern Physics B*, 20 (10) (2006) 1141-1199.
- [17] I. A. H. Hassan, On solving some eigenvalue problems by using a differential transformation, *Applied Mathematics and Computation*, 127 (1) (2002) 1-22.
- [18] J. N. Reddy and S. D. Pang, Nonlocal continuum theories of beams for the analysis of carbon nanotubes, *Journal of Applied Physics*, 103 (2) (2008) 023511.
- [19] H. Jiang, B. Liu, Y. Huang and K. C. Hwang, Thermal expansion of single wall carbon nanotubes, *Journal of Engineering Materials and Technology*, 126 (3) (2004) 265-270.
- [20] X. Yao and Q. Han, Buckling analysis of multiwalled carbon nanotubes under torsional load coupling with temperature change, *Journal of Engineering Materials and Technology*, 128 (3) (2006) 419-427.



**Farzad Ebrahimi** received his B.S., M.S. and Ph.D. degrees in Mech. Eng. from the University of Tehran, Iran. Dr. Ebrahimi is now an assistant professor in the Department of Mech. Eng. at the International University of Imam Khomeini.